4-19-2017

Damage location and quantification of a pretensioned concrete beam using stochastic subspace identification

Alessandro Cancelli
Iowa State University, acancell@iastate.edu

Laura Micheli
Iowa State University, lauramch@iastate.edu

Simon Laflamme
Iowa State University, laflamme@iastate.edu

Alice Alipour
Iowa State University, alipour@iastate.edu

Sri Sritharan
Iowa State University, sri@iastate.edu

See next page for additional authors

Damage location and quantification of a pretensioned concrete beam using stochastic subspace identification

Abstract

Stochastic subspace identification (SSID) is a first-order linear system identification technique enabling modal analysis through the time domain. Research in the field of structural health monitoring has demonstrated that SSID can be used to successfully retrieve modal properties, including modal damping ratios, using output-only measurements. In this paper, the utilization of SSID for indirectly retrieving structures' stiffness matrix was investigated, through the study of a simply supported reinforced concrete beam subjected to dynamic loads. Hence, by introducing a physical model of the structure, a second-order identification method is achieved. The reconstruction is based on system condensation methods, which enables calculation of reduced order stiffness, damping, and mass matrices for the structural system. The methods compute the reduced order matrices directly from the modal properties, obtained through the use of SSID. Lastly, the reduced properties of the system are used to reconstruct the stiffness matrix of the beam. The proposed approach is first verified through numerical simulations and then validated using experimental data obtained from a full-scale reinforced concrete beam that experienced progressive damage. Results show that the SSID technique can be used to diagnose, locate, and quantify damage through the reconstruction of the stiffness matrix.

Keywords

Damage detection, structural health monitoring, stochastic system identification, reduced order, output-only, stiffness reconstruction, vibration-based

Disciplines

Civil Engineering | Structural Engineering | VLSI and Circuits, Embedded and Hardware Systems

Comments

This proceeding is published as Alessandro Cancelli, Laura Micheli, Simon Laflamme, Alice Alipour, Sri Sritharan, Filippo Ubertini, "Damage location and quantification of a pretensioned concrete beam using stochastic subspace identification", Proc. SPIE 10169, Nondestructive Characterization and Monitoring of Advanced Materials, Aerospace, and Civil Infrastructure 2017, 1016917 (19 April 2017); doi: 10.1117/12.2261825. Posted with permission.

Authors

Alessandro Cancelli, Laura Micheli, Simon Laflamme, Alice Alipour, Sri Sritharan, and Filippo Ubertini

Damage location and quantification of a pretensioned concrete beam using stochastic subspace identification

Alessandro Cancelli, Laura Micheli, Simon Laflamme, Alice Alipour, Sri Sritharan, et al.

Alessandro Cancelli, Laura Micheli, Simon Laflamme, Alice Alipour, Sri Sritharan, Filippo Ubertini, "Damage location and quantification of a pretensioned concrete beam using stochastic subspace identification," Proc. SPIE 10169, Nondestructive Characterization and Monitoring of Advanced Materials, Aerospace, and Civil Infrastructure 2017, 1016917 (19 April 2017); doi: 10.1117/12.2261825

Event: SPIE Smart Structures and Materials + Nondestructive Evaluation and Health Monitoring, 2017, Portland, Oregon, United States

Damage location and quantification of a pretensioned concrete beam using stochastic subspace identification

Alessandro Cancelli[a], Laura Micheli[a], Simon Laflamme[a b], Alice Alipour[a], Sri Sritharan[a], Filippo Ubertini[c]

[a] Dep. of Civil, Construction and Environmental Engineering, Iowa State University, 813 Bissel Road, Ames, IA, USA 50011-1066; [b] Dep. Of Electrical and Computer Engineering, Iowa State University, 2215 Coover Hall, Ames, IA, USA 50011-3060; [c] Dep. Of Civil and Environmental Engineering, University of Perugia, 83 Goffredo Duranti Street, Perugia, Italy 06125

ABSTRACT

Stochastic subspace identification (SSID) is a first-order linear system identification technique enabling modal analysis through the time domain. Research in the field of structural health monitoring has demonstrated that SSID can be used to successfully retrieve modal properties, including modal damping ratios, using output-only measurements. In this paper, the utilization of SSID for indirectly retrieving structures' stiffness matrix was investigated, through the study of a simply supported reinforced concrete beam subjected to dynamic loads. Hence, by introducing a physical model of the structure, a second-order identification method is achieved. The reconstruction is based on system condensation methods, which enables calculation of reduced order stiffness, damping, and mass matrices for the structural system. The methods compute the reduced order matrices directly from the modal properties, obtained through the use of SSID. Lastly, the reduced properties of the system are used to reconstruct the stiffness matrix of the beam. The proposed approach is first verified through numerical simulations and then validated using experimental data obtained from a full-scale reinforced concrete beam that experienced progressive damage. Results show that the SSID technique can be used to diagnose, locate, and quantify damage through the reconstruction of the stiffness matrix.

Keywords: Damage detection, structural health monitoring, stochastic system identification, reduced order, output-only, stiffness reconstruction, vibration-based.

1. INTRODUCTION

The field of structural health monitoring (SHM) is attracting research on methods enabling damage diagnosis, localization, and prognosis for civil infrastructure. Different algorithms have been proposed and evaluated, but SHM is yet to be widely accepted and implemented, likely due to the lack of integrated SHM systems capable of automatically yielding information to directly conduct condition assessment-driven decisions.

There have been vast efforts in developing vibration-based SHM methods[1-3] due to the ease of installation and deployment of vibration measurement devices such as accelerometers. Vibration-based SHM typically links damage with changes in natural frequencies and mode shapes of the structure. A challenge in vibration-based condition assessment reside in the clear detection of small changes in modal properties that are caused by a specific damage. Another challenge with this assessment is identification of the location and quantification of such damage once a change in the modal properties has been detected. This task is further complicated under changing environmental conditions, due to effects of temperature and humidity on modal properties.

Stochastic subspace identification (SSID) is an output only modal identification technique that has shown some promise in accurately detecting modal properties, even in presence of closely spaced modes and non-classically damped systems, including highly damped ones. SSID-based methods are typically output-only approaches[4] that can be used to extract modal properties of a given structure from time-domain data. They can be divided[5] in covariance-driven (SSID-COV) and data-driven (SSID-DATA) methods. The latter are of particular interest in the analysis of real structures since they use a limited set of reference sensors to obtain a faster identification. Peeters[6] used this approach for both laboratory test and real structures monitoring, obtaining promising results for damage detection. However, this method requires user intervention to extract the modal properties of the analyzed system. The automation of SSID has been studied by Andersen[7] *et al.* and Ubertini[8] *et al.*, who proposed a clustering-based approach to rapidly extract modal properties of the structures.

Nondestructive Characterization and Monitoring of Advanced Materials, Aerospace, and Civil Infrastructure 2017,
edited by H. Felix Wu, Andrew L. Gyekenyesi, Peter J. Shull, Tzu-Yang Yu, Proc. of SPIE Vol. 10169,
1016917 · © 2017 SPIE · CCC code: 0277-786X/17/$18 · doi: 10.1117/12.2261825

This method was applied to two real case studies, obtaining promising results in the optic of permanent monitoring of the structure. Examples of SSID applications to full-scale bridge structures is found in Refs.[9, 10], where the technique was applied to the Z24 Bridge in Switzerland[9] and the Tamar Bridge[10] in the UK. More recently SSID has been applied for vibration-based SHM of the monumental San Pietro bell-tower in Perugia, Italy[11].

This paper investigates the use of SSID-based modal data to reconstruct stiffness matrices, from which damage could be diagnosed, located, and quantified through spatiotemporal comparison of data. These matrices could also be used to update physical models of a given structure. It uses incomplete modal information, retrieved from output-only data, to build reduced order stiffness matrices of the structure. The algorithm is divided into two sequential phases. First, the modal information (i.e., frequencies and modes shapes) of the structure are retrieved from the output data using the SSID method. In the second phase, the reduced order matrices of the system are built directly from the modal information and then used to design specific optimization functions. A swarm optimization algorithm is used to analyze these functions to locate the damage. The algorithm is verified through numerical simulations and validated on experimental data obtained from a full-scale, simply supported, precast, pretensioned concreter (PC) beam subjected to white noise excitation.

The rest of the paper is organized as follows. Section 2 provides the theoretical background on the SSID technique and the reduced order matrices derivation. Section 3 introduces the two-phase algorithm. Sections 4 and 5 present and discuss results from the numerical simulations and the full-scale test, respectively. Section 6 concludes the paper.

2. BACKGROUND

2.1 Stochastic subspace identification

The stochastic subspace identification (SSID) technique is a dynamic systems analysis tool used to retrieve natural frequencies, mode shapes and modal damping. These dynamic properties are extracted from a linear state space representation reconstructed directly from measured data. Consider the discrete-time state space representation[12]:

$$\begin{aligned} \mathbf{x}_{k+1} &= \mathbf{A}\mathbf{x}_k + \mathbf{w}_k \\ \mathbf{y}_k &= \mathbf{C}\mathbf{x}_k + \mathbf{v}_k \end{aligned} \tag{1}$$

where the subscript k indicates a discrete step; $\mathbf{x}$ is the state vector; $\mathbf{A}$ is the state matrix; $\mathbf{y}$ is the output vector; $\mathbf{C}$ is the output matrix; $\mathbf{w}$ and $\mathbf{v}$ are zero-mean Gaussian stationary process, whereby the former models the identification process noise and the unknown excitation while the latter models the signal noise. Both Gaussian processes are defined by their covariance matrix $\mathbf{\Sigma}$:

$$\mathbf{\Sigma} = \begin{bmatrix} \mathbf{Q}_w & \mathbf{S}_{w,v} \\ \mathbf{S}_{w,v}^{\mathrm{T}} & \mathbf{R}_v \end{bmatrix} \tag{2}$$

where $\mathbf{Q}_w$ is the variance matrix of $\mathbf{w}$; $\mathbf{R}_v$ is the variance matrix of $\mathbf{v}$, and $\mathbf{S}_{w,v}$ is the covariance matrix between the two Gaussian processes.

The procedure to retrieve the dynamic parameters of the system is as follows[5]: a block Henkel matrix $\mathbf{H}$ is built using outputs $\mathbf{y}_k$ from step k and $\mathbf{y}_{k+1}$ from step $k+1$. The resulting matrix is composed of two submatrices $\mathbf{Y}_p$ and $\mathbf{Y}_f$, usually termed as *past* and *future*. Both submatrices have i block rows and j columns, with $j \le s - 2i + 1$ and s is the total number of time samples available. The range for the two parameters i and j is defined by the user before the analysis.

$$\mathbf{H} = \left(\frac{\mathbf{Y}_p}{\mathbf{Y}_f} \right) . \tag{3}$$

The block Henkel matrix is decomposed using the QR-factorization:

$$\mathbf{H} = \left(\frac{\mathbf{Y}_p}{\mathbf{Y}_f} \right) = \mathbf{R}\mathbf{Q}^{\mathbf{T}} \tag{4}$$

where **Q** is a square orthonormal matrix of dimension j such that $\mathbf{Q}^{\mathrm{T}}\mathbf{Q} = \mathbf{Q}\mathbf{Q}^{\mathrm{T}} = \mathbf{I}_j$, $\mathbf{I}_j$ is the identity matrix of dimension j, and **R** is a lower triangular matrix of dimension $l \times j$ with l being the total number of sensors. Using the decomposition of the Henkel matrix, a projection $\mathcal{P}_i$ of the past row space into the future row space is computed as:

$$\mathcal{P}_i = \mathbf{Y}_f / \mathbf{Y}_p = \mathbf{Y}_f \mathbf{Y}_p^{\mathrm{T}} \left(\mathbf{Y}_p \mathbf{Y}_p^{\mathrm{T}} \right)^{\dagger} \mathbf{Y}_p = \begin{bmatrix} \mathbf{R}_{21} \\ \mathbf{R}_{31} \\ \mathbf{R}_{41} \end{bmatrix} \mathbf{Q}_1^{\mathrm{T}} \tag{5}$$

where $(\bullet)^{\dagger}$ is the Moore-Penrose pseudo-inverse of a matrix, $\mathbf{R}_{21}$, $\mathbf{R}_{31}$, $\mathbf{R}_{41}$ are submatrices of **R** and $\mathbf{Q}_1$ is a submatrix of **Q**. The projection is expressed as a product between the observability matrix of the system $\mathbf{O}_i$ and a Kalman filter state sequence $\hat{\mathbf{X}}_i$:

$$\mathcal{P}_i = \begin{bmatrix} \mathbf{C} \\ \mathbf{CA} \\ \mathbf{CA}^2 \\ \ldots \\ \mathbf{CA}^{i-1} \end{bmatrix} \begin{bmatrix} \hat{\mathbf{x}}_i & \hat{\mathbf{x}}_{i+1} & \ldots & \hat{\mathbf{x}}_{i+j-1} \end{bmatrix} = \mathbf{O}_i \hat{\mathbf{X}}_i . \tag{6}$$

Both the observability matrix and the Kalman filter state sequence are retrieved through singular value decomposition (SVD) of the projection:

$$\mathcal{P}_i = \mathbf{U}\mathbf{S}\mathbf{V}^{\mathbf{T}} \tag{7}$$

$$\mathbf{O}_i = \mathbf{U}\mathbf{S}^{1/2} \tag{8}$$

$$\hat{\mathbf{X}}_i = \mathbf{O}_i^{\dagger} \mathcal{P}_i \tag{9}$$

where **U**, **S** and **V** are the matrices obtained from the SVD of the projection. An overdetermined set of linear equations is obtained from the estimated Kalman filter state sequence as follow:

$$\begin{bmatrix} \hat{\mathbf{X}}_{i+1} \\ \mathbf{Y}_i \end{bmatrix} = \begin{bmatrix} \mathbf{A} \\ \mathbf{C} \end{bmatrix} \hat{\mathbf{X}}_i + \begin{pmatrix} \boldsymbol{\rho}_w \\ \boldsymbol{\rho}_v \end{pmatrix} \tag{10}$$

where $\mathbf{Y}_i$ is an Henkel matrix with only one row block, $\boldsymbol{\rho}_w$ and $\boldsymbol{\rho}_v$ are the residual respectively of the modelling noise and the data noise; **A** and **C** are obtained from a least square solution of this overdetermined problem:

$$\begin{bmatrix} \mathbf{A} \\ \mathbf{C} \end{bmatrix} = \begin{bmatrix} \hat{\mathbf{X}}_{i+1} \\ \mathbf{Y}_i \end{bmatrix} \hat{\mathbf{X}}_i^{\dagger} . \tag{11}$$

These retrieved matrices are expressed in discrete-time form; in particular **A** can be decomposed through eigenvalues and eigenvectors to obtain:

$$\mathbf{A} = \mathbf{\Psi}_d \mathbf{\Lambda}_d \mathbf{\Psi}_d^{-1} \tag{12}$$

$$\mathbf{\Lambda}_d = \begin{bmatrix} \lambda_{d,1} & 0 & \cdots & 0 \\ 0 & \lambda_{d,2} & \cdots & 0 \\ \vdots & \vdots & \ddots & \vdots \\ 0 & 0 & \cdots & \lambda_{d,n} \end{bmatrix} \tag{13}$$

where $\mathbf{\Lambda}_d$ is a diagonal matrix containing the $\lambda_{d,1}$, $\lambda_{d,2}$, …, $\lambda_{d,n}$ discrete time complex eigenvalues and $\mathbf{\Psi}_d$ is the discrete time complex eigenvector matrix. These discrete time quantities are converted into continuous time quantities to obtain the dynamic parameters of the system:

$$\mathbf{A} = e^{\mathbf{A}_c \Delta t} \tag{14}$$

$$\mathbf{C}_c = \mathbf{C} \tag{15}$$

$$\boldsymbol{\lambda}_c = \frac{\ln\left(\boldsymbol{\lambda}_d\right)}{\Delta t} \tag{16}$$

$$\mathbf{\Psi}_c = \mathbf{\Psi}_d \tag{17}$$

where the subscript d indicates discrete-time quantities, the subscript c indicates continuous time quantities, $\boldsymbol{\lambda}$ is a vector containing the complex eigenvalues and Δt is the time step of the measured data. The circular frequencies ω_i and modal damping ξ_i of the system can be determined using the complex conjugates eigenvalues of the matrix $\mathbf{A}_c$:

$$\lambda_{c,i}, \lambda_{c,i}^{*} = -\xi_i \omega_i \pm \boldsymbol{j} \omega_i \sqrt{1-\xi_i^2} \tag{18}$$

where the superscript * indicates the complex conjugate and $\boldsymbol{j}$ is the imaginary unit. Lastly, the mode shapes matrix $\mathbf{\Phi}$ of the system can be obtained from the continuous time eigenvectors $\mathbf{\Psi}_d$:

$$\mathbf{\Phi} = \mathbf{C}_c \mathbf{\Psi}_c . \tag{19}$$

It follows that the dynamic properties of the structural system can be derived from the retrieved discrete-time matrices **A** and **C**. However, the order of the system, or the dimension of the aforementioned matrices **A** and **C**, is generally unknown. To obtain the modal information of the system it is necessary to analyze a wide range of the parameters i and j. For this purpose, Ubertini[8] *et al*. developed an automated modal identification procedure divided in three steps. First, the complex conjugates eigenvalues are eliminated from the results. Then, specific control criteria for frequencies, damping, and mode shapes are used to eliminate modes created from the noise of the identification process and from overmodelling. Finally, the remaining modes are clustered and the structure's modal information are chosen by analyzing the stability of these modes (similarity of the parameters in the various model order and number of output block rows of the block Henkel matrix).

2.2 Condensation Methods

In the approach, the physical system is simplified into a finite element model of degrees-of-freedom (DOFs) equal to the number of sensors. This yields a reduced order model, dynamic properties of which can be obtained from the SSID method. Here, two different system reduction techniques[13] are employed to locate and quantify the damage. The first technique is the Guyan reduction used for static condensation. This yields a modified stiffness matrix used for the identification of changes in physical parameters. The second technique is the system equivalent reduction expansion process (SEREP), used for dynamic condensation. This allows for the temporal comparison of dynamic properties, leading to the quantification of changes in stiffness. Both methods are used in the proposed algorithm to create different performance metrics and improve the precision of the reconstructed stiffness of the system. The following two subsections provide a background on the condensation methods.

2.2.1 Guyan (static) condensation method

The dynamics of a physical model can be described by the matrix form of the equation of motion[12]:

$$\mathbf{M}\ddot{\mathbf{x}}+\mathbf{C}\dot{\mathbf{x}}+\mathbf{K}\mathbf{x}=\mathbf{F}(t) \tag{20}$$

where $\mathbf{M}$ is the mass matrix, $\mathbf{C}$ is the damping matrix, $\mathbf{K}$ is the stiffness matrix, $\mathbf{F}(t)$ is forcing matrix, $\mathbf{x}$ is the displacement vector, and the dot denotes a time derivative.

Eq. (20) can be divided in terms associated with the measured DOFs, m, and the complementary DOFs, c:

$$\begin{bmatrix}\mathbf{M}_{mm} & \mathbf{M}_{mc}\\ \mathbf{M}_{cm} & \mathbf{M}_{cc}\end{bmatrix}\begin{bmatrix}\ddot{\mathbf{x}}_m\\ \ddot{\mathbf{x}}_c\end{bmatrix}+\begin{bmatrix}\mathbf{C}_{mm} & \mathbf{C}_{mc}\\ \mathbf{C}_{cm} & \mathbf{C}_{cc}\end{bmatrix}\begin{bmatrix}\dot{\mathbf{x}}_m\\ \dot{\mathbf{x}}_c\end{bmatrix}+\begin{bmatrix}\mathbf{K}_{mm} & \mathbf{K}_{mc}\\ \mathbf{K}_{cm} & \mathbf{K}_{cc}\end{bmatrix}\begin{bmatrix}\mathbf{x}_m\\ \mathbf{x}_c\end{bmatrix}=\begin{bmatrix}\mathbf{F}_m(t)\\ \mathbf{F}_c(t)\end{bmatrix}. \tag{21}$$

Assuming a static behavior, which eliminates the inertia and damping terms, and assuming that no forces are applied to the complementary DOFs, the equation reduces to:

$$\begin{bmatrix}\mathbf{K}_{mm} & \mathbf{K}_{mc}\\ \mathbf{K}_{cm} & \mathbf{K}_{cc}\end{bmatrix}\begin{bmatrix}\mathbf{x}_m\\ \mathbf{x}_c\end{bmatrix}=\begin{bmatrix}\mathbf{F}_m(t)\\ \mathbf{0}\end{bmatrix}. \tag{22}$$

Solving for $\mathbf{x}_c$ one obtains:

$$\mathbf{x}_c=-\mathbf{K}_{cc}^{-1}\mathbf{K}_{cm}\mathbf{x}_m \tag{23}$$

Substituting Eq. (23) in the top row Eq. (22) and noting that $\mathbf{K}_{mc}$=$\mathbf{K}_{cm}$ yield a reduced order stiffness matrix $\overline{\mathbf{K}}_{\mathrm{red,G}}$:

$$\overline{\mathbf{K}}_{\mathrm{red,G}}=\mathbf{K}_{mm}-\mathbf{K}_{mc}\mathbf{K}_{cc}^{-1}\mathbf{K}_{mc}^{\mathrm{T}}. \tag{24}$$

To obtain a relation between $\overline{\mathbf{K}}_{\mathrm{red,G}}$ and the modal properties of the system, one must assume the absence of rigid body modes[14]. This assumption leads to an invertible eigenvalues matrix $\mathbf{\Omega}$ that can be used to decompose the inverse of the stiffness matrix:

$$\mathbf{K}^{-1}=\mathbf{\Phi}\,\mathbf{\Omega}^{-1}\mathbf{\Phi}^{\mathrm{T}} \tag{25}$$

$$\mathbf{\Omega}=\begin{bmatrix}\lambda_1 & 0 & \cdots & 0\\ 0 & \lambda_2 & \cdots & 0\\ \vdots & \vdots & \ddots & \vdots\\ 0 & 0 & \cdots & \lambda_n\end{bmatrix} \tag{26}$$

where n is the total number of system DOFs, $\mathbf{\Phi}$ is the eigenvectors matrix, $\mathbf{\Omega}$ is the diagonal eigenvalues matrix, $\lambda_i = \omega_i^2$ and ω_i is the i^{th} mode circular frequency.

Rearranging Eq. (25) with the partition of $\mathbf{K}$ shown in Eq. (22), the inverse stiffness matrix can be written as follows:

$$\mathbf{K}^{-1} = \begin{bmatrix} \bar{\mathbf{K}}_{\text{red,G}}^{-1} & -\bar{\mathbf{K}}_{\text{red,G}}^{-1}\mathbf{K}_{cm}\mathbf{K}_{cc}^{-1} \\ -\mathbf{K}_{cc}^{-1}\mathbf{K}_{mc}^{\text{T}}\bar{\mathbf{K}}_{\text{red,G}}^{-1} & \mathbf{K}_{cc}^{-1}\left(\text{I}+\mathbf{K}_{mc}^{\text{T}}\bar{\mathbf{K}}_{\text{red,G}}^{-1}\mathbf{K}_{cm}\mathbf{K}_{cc}^{-1}\right) \end{bmatrix}. \tag{27}$$

Consider the following coordinate change:

$$\mathbf{x}(t) = \begin{bmatrix} \mathbf{x}_m(t) \\ \mathbf{x}_c(t) \end{bmatrix} = \mathbf{\Phi}\,\mathbf{q}(t) = \begin{bmatrix} \mathbf{\Phi}_m \\ \mathbf{\Phi}_c \end{bmatrix}\mathbf{q}(t) \tag{28}$$

where $\mathbf{x}$ and $\mathbf{q}$ are associated with the physical and modal coordinates of the system, respectively, $\mathbf{\Phi}_m$ is a matrix containing the eigenvectors of the measured DOFs and $\mathbf{\Phi}_c$ is a matrix containing the eigenvectors of the complementary DOFs. Substituting Eq. (28) into Eq. (25) gives:

$$\mathbf{K}^{-1} = \begin{bmatrix} \mathbf{\Phi}_m\mathbf{\Omega}^{-1}\mathbf{\Phi}_m^{\text{T}} & \mathbf{\Phi}_m\mathbf{\Omega}^{-1}\mathbf{\Phi}_c^{\text{T}} \\ \mathbf{\Phi}_c\mathbf{\Omega}^{-1}\mathbf{\Phi}_m^{\text{T}} & \mathbf{\Phi}_c\mathbf{\Omega}^{-1}\mathbf{\Phi}_c^{\text{T}} \end{bmatrix}. \tag{29}$$

Comparing Eq. (30) with Eq. (28) yields an expression for $\bar{\mathbf{K}}_{\text{red,G}}$ function of the modal properties of the system:

$$\bar{\mathbf{K}}_{\text{red,G}} = \left(\mathbf{\Phi}_m\mathbf{\Omega}^{-1}\mathbf{\Phi}_m^{\text{T}}\right)^{-1}. \tag{30}$$

Eq. (30) can be used to associate changes in dynamic properties to changes in stiffness. However, the quality of the eigenvalues approximation highly depends on the location of the sensors.

2.2.2 System equivalent reduction expansion process (SEREP) condensation method

An expression for the modal coordinates using a least square estimator can be derived from the first row of Eq. (28):

$$\mathbf{q} = \mathbf{\Phi}_m^{\dagger}\mathbf{x}_m. \tag{31}$$

Substituting (31) in (28) yields the transformation matrix for the SEREP approach:

$$\mathbf{x} = \mathbf{\Phi}\mathbf{\Phi}_m^{\dagger}\mathbf{x}_m = \mathbf{T}_r\mathbf{x}_{\text{m}} \tag{32}$$

$$\mathbf{T}_r = \mathbf{\Phi}\mathbf{\Phi}_m^{\dagger}. \tag{33}$$

Using Eq. (33) in (20) and pre-multiplying all the terms of the resulting equation by $\mathbf{T}_r^{\text{T}}$ leads to:

$$\mathbf{T}_r^{\text{T}}\mathbf{M}\mathbf{T}_r\ddot{\mathbf{x}}_m + \mathbf{T}_r^{\text{T}}\mathbf{C}\mathbf{T}_r\dot{\mathbf{x}}_m + \mathbf{T}_r^{\text{T}}\mathbf{K}\mathbf{T}_r\mathbf{x}_m = \mathbf{T}_r^{\text{T}}\mathbf{F}(t). \tag{34}$$

Expanding the part of the equation that is relative to the stiffness matrix and noting that $\mathbf{\Phi}^{\text{T}}\mathbf{K}\mathbf{\Phi} = \mathbf{\Omega}^2$, one obtains an expression for $\bar{\mathbf{K}}_{\text{red,S}}$:

$$\bar{\mathbf{K}}_{\text{red,S}} = \mathbf{T}_r^{\text{T}}\mathbf{K}\mathbf{T}_r = \left(\mathbf{\Phi}_m^{\dagger}\right)^{\text{T}}\mathbf{\Phi}^{\text{T}}\mathbf{K}\mathbf{\Phi}\mathbf{\Phi}_m^{\dagger} = \left(\mathbf{\Phi}_m^{\dagger}\right)^{\text{T}}\mathbf{\Omega}^2\mathbf{\Phi}_m^{\dagger}. \tag{35}$$

This condensation method preserves the selected eigenvalues of the original system through the transformation, implying that the selected mode's eigenvalues are equal for both systems. This property is independent of the location and the number of sensors.

3. DAMAGE DETECTION ALGORITHM

The proposed damage detection, location, and quantification method is divided into two sequential stages. First, accelerations data are analyzed using the SSID technique to extract the natural frequencies and mode shapes of the monitored system. This information is used to calculate the reduced order stiffness matrices of the system, after proper normalization of the mode shapes. Second, the modal properties and reduced order stiffness matrices are compared with the properties of the physical model. This comparison is conducted through three optimization functions, which are solved using a particle swarm algorithm[15]. Results of this optimization process are used to detect, locate, and quantify damage.

3.1 Stage I – Extraction of modal properties

Here, the system's frequencies, $\boldsymbol{f}_{retr}$, and mode shapes, $\boldsymbol{\Phi}_{retr}$, are extracted through the SSID technique. This is achieved through the three-step method proposed by Ubertini[8], which was very effective in removing all the spurious modes generated from the noise inherent in the identification process and from overmodelling errors. Figure 1 shows typical raw data obtained from an SSID analysis using laboratory data from this work (to be described later), while figure 2 shows the same data after filtering out the noisy modes. One can observe that after filtering, the first frequency of the system became immediately identifiable as the only stable frequency in the 0-10 Hz range. Clustering was used to identify the higher modes. The technique consists of aggregating the remaining modes into clusters that meet predefined criteria. The structural modes can be selected by analyzing the mode shapes of the clustered sets. Figure 3 shows an example of the clustering process results for the stable modes of the system (Figure 2), showing the 90% confidence interval for the damping (vertical lines) and the frequencies (horizontal lines). The first three identified modes of the system are circled in the figure, where one intermediary mode (around 38 Hz) was not considered as it was associated with high damping. The retrieved frequencies and mode shapes were used to calculate $\overline{\mathbf{K}}_{red,G,data}$ (Eq. (30)) and $\overline{\mathbf{K}}_{red,S,data}$ (Eq. (35)).

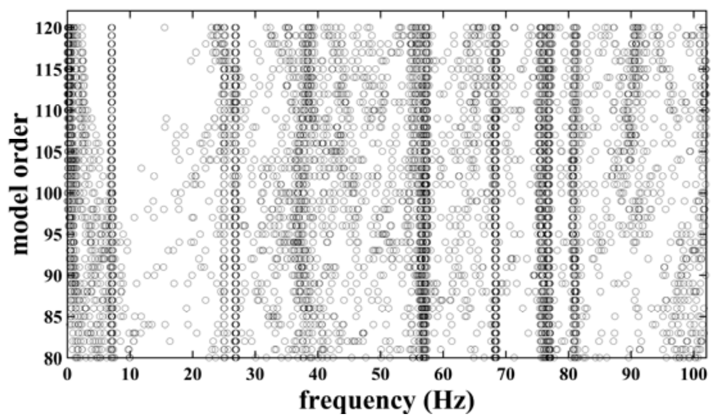

Figure 1. Retrieved frequencies versus model order *i* identified by the SSID algorithm before the elimination of noisy modes.

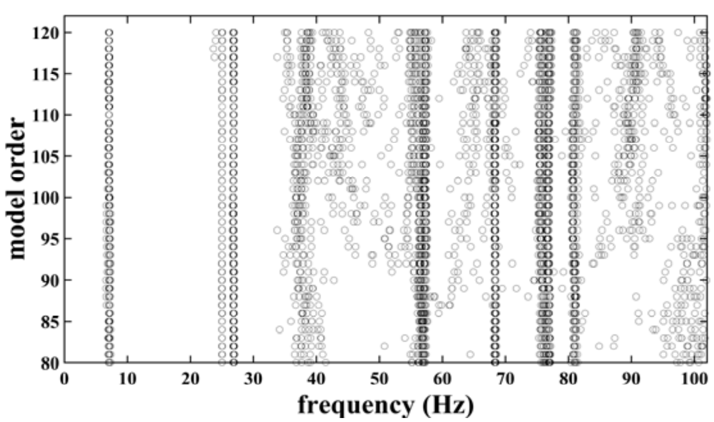

Figure 2. Retrieved frequencies versus model order *i* identified by the SSID algorithm after the elimination of noisy modes.

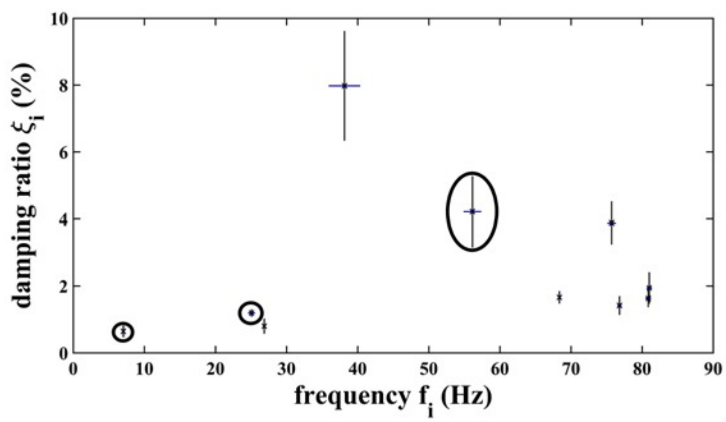

Figure 3. Retrieved frequencies versus damping ratios after the clustering process, showing the identified system modes encircled.

3.2 Stage II – Damage detection and location

In this stage, a finite element model of the structure is constructed, containing parameters that can be altered as a function of damage indices, α_i. These indices multiply the bending stiffness *EI* of the model's elements, where *E* is the Young's modulus of the material and *I* is the sections' moment of inertia that can differ between elements. Parameters α_i are selected based on an optimization function, which yield to an updated finite element model from which the model-driven dynamic parameters and reduced order matrices can be obtained.

Three different optimization functions are used to select parameters α_i, each solved independently, thus yielding three different sets of damage indices. These optimization functions are based on four performance indices J_1 to J_4. They are defined as follows:

- Index J_1: the mean absolute percentage error between the retrieved frequencies and the frequencies obtained from the model.

$$J_1 = \frac{1}{\mathrm{N}_d} \sum_{d=1}^{\mathrm{N}_d} \left(\frac{\left(f_{\mathrm{retr},d} - f_{\mathrm{func},d} \right)}{f_{\mathrm{retr},d}} 100 \right) \tag{36}$$

  where N_d is the number of selected frequencies, $f_{\mathrm{retr},d}$ is the d^{th} retrieved frequency and $f_{\mathrm{funct},d}$ is the d^{th} frequency obtained from the model.

- Index J_2: the mean value of the standard deviation for the ratio of the computed and retrieved mode shapes.

$$J_2 = \frac{1}{\mathrm{N}_d} \sum_{d=1}^{\mathrm{N}_d} \left(\frac{1}{\left(\mathrm{N}_s - 1 \right)} \sum_{s=1}^{\mathrm{N}_s} \left(\Phi_{ds,\mathrm{rt}} - \bar{\Phi}_{d,\mathrm{rt}} \right)^2 \right) \tag{37}$$

$$\Phi_{ds,\mathrm{rt}} = \frac{\Phi_{\mathrm{funct},ds}}{\Phi_{\mathrm{retr},ds}} \tag{38}$$

$$\bar{\Phi}_{d,\mathrm{rt}} = \frac{1}{\mathrm{N}_s} \sum_{s=1}^{\mathrm{N}_s} \left(\frac{\Phi_{\mathrm{funct},ds}}{\Phi_{\mathrm{retr},ds}} \right) \tag{39}$$

where N_s is the number of sensors, $\Phi_{funct,ds}$ is the s^{th} component of the d^{th} mode shape function and $\Phi_{retr,ds}$ is the s^{th} component of the d^{th} retrieved mode shape.

- Index J_3: the mean of the absolute value of all the terms in the Guyan error matrix. This matrix is defined as the absolute percentage error between the elements of the retrieved and the model's Guyan reduced order stiffness matrices.

$$J_3 = \frac{1}{N_s}\sum_{s=1}^{N_s}\left(\frac{1}{N_s}\sum_{z=1}^{N_s}\left(K_{G,diff,sz}\right)\right) \tag{40}$$

$$K_{G,diff,sz} = \left|\frac{\bar{K}_{red,G,data,sz} - \bar{K}_{red,G,funct,sz}}{\bar{K}_{red,G,data,sz}}100\right| \tag{41}$$

where $\bar{K}_{red,G,data,sz}$ and $\bar{K}_{red,G,funct,sz}$ are the elements in position *sz* of the retrieved and model's Guyan matrices, respectively.

- Index J_4: the mean of the absolute value of all the terms in the SEREP error matrix. This matrix is defined as the absolute percentage error between the elements of the retrieved and the model's SEREP reduced order stiffness matrices

$$J_4 = \frac{1}{N_s}\sum_{s=1}^{N_s}\left(\frac{1}{N_s}\sum_{z=1}^{N_s}\left(K_{S,diff,sz}\right)\right) \tag{42}$$

$$K_{S,diff,sz} = \left|\frac{\bar{K}_{red,S,data,sz} - \bar{K}_{red,S,funct,sz}}{\bar{K}_{red,S,data,sz}}100\right| \tag{43}$$

where $\bar{K}_{red,S,data,sz}$ and $\bar{K}_{red,S,funct,sz}$ are the elements in position *sz* of the retrieved and model's SEREP matrices, respectively.

The three optimization functions consist of minimizing the product of different performance indices, defined as follows:

$$OF_1 = J_1 J_2 J_3 \tag{44}$$

$$OF_2 = J_1 J_2 J_4 \tag{45}$$

$$OF_3 = J_1 \,. \tag{46}$$

These functions are solved using a particle swarm optimization algorithm. The particle swarm optimization algorithm[15] analyzes the evolution of the swarm through successive generation, keeping track in each generation of the best position for the whole swarm and each single particle. The best position is defined as the value that gives a local minima for the analyzed function. This information, in each generation, is used to create the next generation of the swarm in order to obtain a smaller value for the optimization function. The optimization process continues until the value of the function reaches a stable minimum value. Figure 4 shows an example of this optimization process for OF_1 using data from the laboratory experiment (to be described later). As the successive generations of the swarm are created, the value of the function OF_1 decreases until it reaches a stable value.

Damage detection, location, and quantification is conducted by comparing all three sets of α_i selected by the particle optimization swarm. To detect damage, all of the three α_i for a given element need to be below unity, where unity is associated with undamaged condition. If all α_i are different than unity for a given element, then damage is considered to be associated with that element, identifying the damage location. The quantification of damage corresponds to the average value of α_i for that particular element. For example, an average value of α_i= 0.6 would signify an element at 60% of its original health, or 40% damaged.

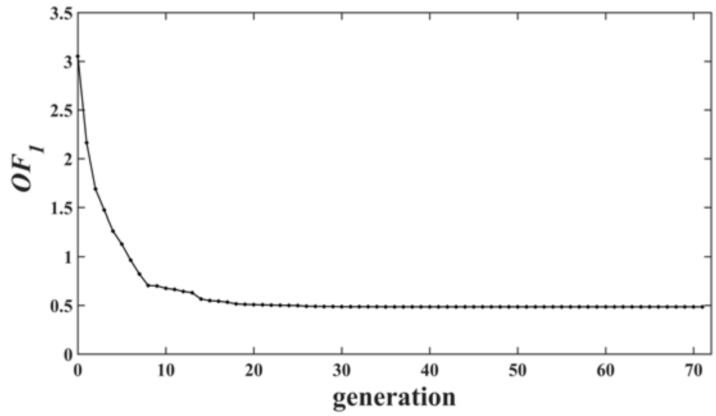

Figure 4. Swarm particle optimization for the first optimization function.

4. ALGORITHM PERFORMANCE ON SIMULATED DATA

The proposed approach was verified on a simulated system, consisting of a simply supported reinforced concrete (RC) beam of 42.5 ft. length. The beam was discretized into 16 elements, as illustrated in figure 5, of constant rectangular cross-sections of 11.8 × 23.6 in^2. Damage was introduced in the system in the form of a reduced moment of inertia for elements 7 and 8 by 20 and 30 %, respectively. This damage entity was chosen as representative of cracks appearing in the elements.

The beam was excited with a white noise excitation between elements 5 and 6 (shown by F(t), figure 5), and the corresponding structural response was taken at three locations to simulate three sensors (numerical locations 1, 2, and 3 in figure 5). Figure 5 shows plots of typical excitation and a corresponding measured acceleration time series.

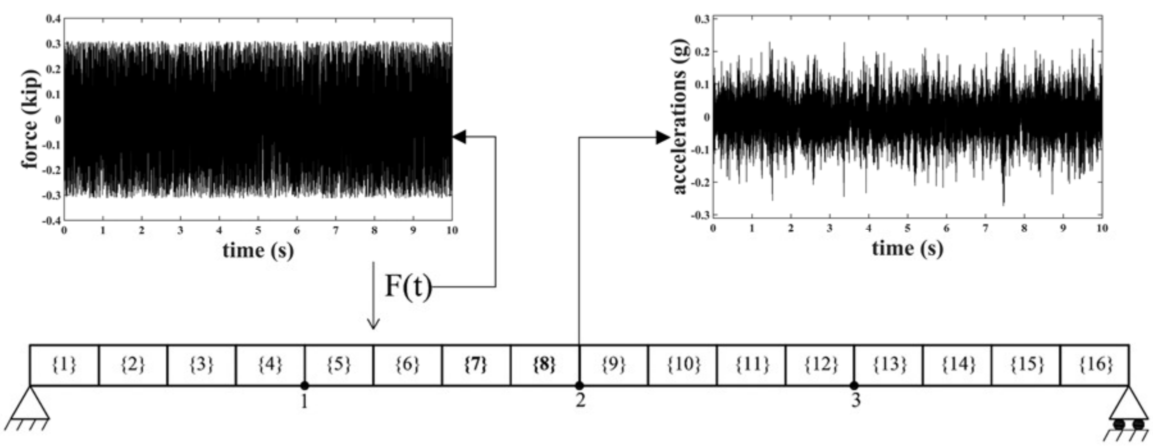

Figure 5. Model of the simulated simply supported RC girder with indication for the element discretization, sensors locations, and force and acceleration response sample.

The SSID algorithm was used to extract modal properties using output-only data. Results for the first four modes are listed in Table 1. Results show good agreement between the model-driven and data-driven modes.

Table 1. First four frequencies of the system, retrieved with SSID and calculated from the model.

Mode	Model frequency (Hz)	SSID frequency (Hz)	Error (%)
1	5.51	5.49	-0.39
2	22.79	22.85	0.29
3	50.18	49.98	-0.39
4	90.28	90.88	0.67

The three sets of damage indices, α_i, retrieved from the particle optimization swarm algorithm are listed in Table 2. Results show that only elements 7 and 8 obtained damage indices α_i values smaller than unity for all of the three optimization functions (OF_i). The average α_i values for elements 7 and 8 were $\alpha_7 = 0.8$ and $\alpha_8 = 0.7$, respectively, which correspond to the simulated damage of 20% and 30%.

Table 2. Damage indices α_i obtained from the particle swarm analysis for the three optimization functions.

Element number	OF_1 α_i	OF_2 α_i	OF_3 α_i
1	1	1	1
2	1	1	1
3	1	1	1
4	1	1	0.95
5	1	1	1
6	1	1	1
7	**0.8**	**0.76**	**0.84**
8	**0.64**	**0.67**	**0.79**
9	1	1	0.75
10	1	1	0.93
11	1	1	1
12	1	1	1
13	0.86	0.85	1
14	1	1	1
15	1	1	1
16	1	1	0.96

5. ALGORITHM PERFORMANCE ON LABORATORY DATA

The algorithm was validated using experimental data obtained from a vibration test on a PC girder. In what follows, the test configuration is described, and the results are presented and discussed.

5.1 Specimen and test description

The specimen tested, identified as BTC60, consisted of a girder and a partial deck over the mid-span. The beam was a standard, pretensioned bulb-tee type C girder designed by Iowa Department of Transportation with a depth of 45 in. This specimen was part of a larger set of experiments conducted for the NCHRP project 12-94 with minimum longitudinal reinforcement. The simply supported span of the beam was 60 ft. with a partial deck extending symmetrically about the mid-span for a length of 22.3 ft. Figure 6 shows the cross-sectional dimensions of both the girder (figure 6(a)) and composite (figure 6(b)) sections.

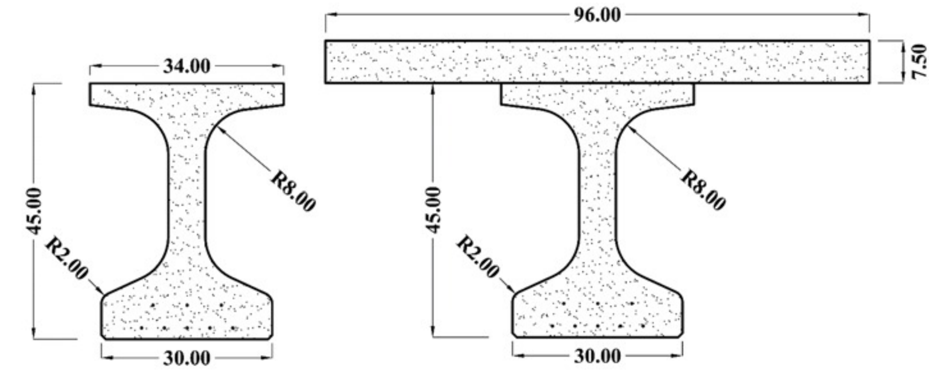

(a) (b)

Figure 6. BTC60 (a) girder and (b) composite cross sections schematics (all dimensions in inches).

The test beam was excited using an RMK-2200 servo hydraulic shaker, controlled through LabVIEW environment, applying a white noise excitation over 80 sec. For safety reasons, chains were used to loosely connect the beam supports to the end sections of the beam (Figure 7). The response of the structure was collected using nine accelerometers mounted to the bottom surface of the girder, and one additional accelerometer was mounted to the top of the actuator. Figure 7 shows the distribution of the sensors and the shaker location.

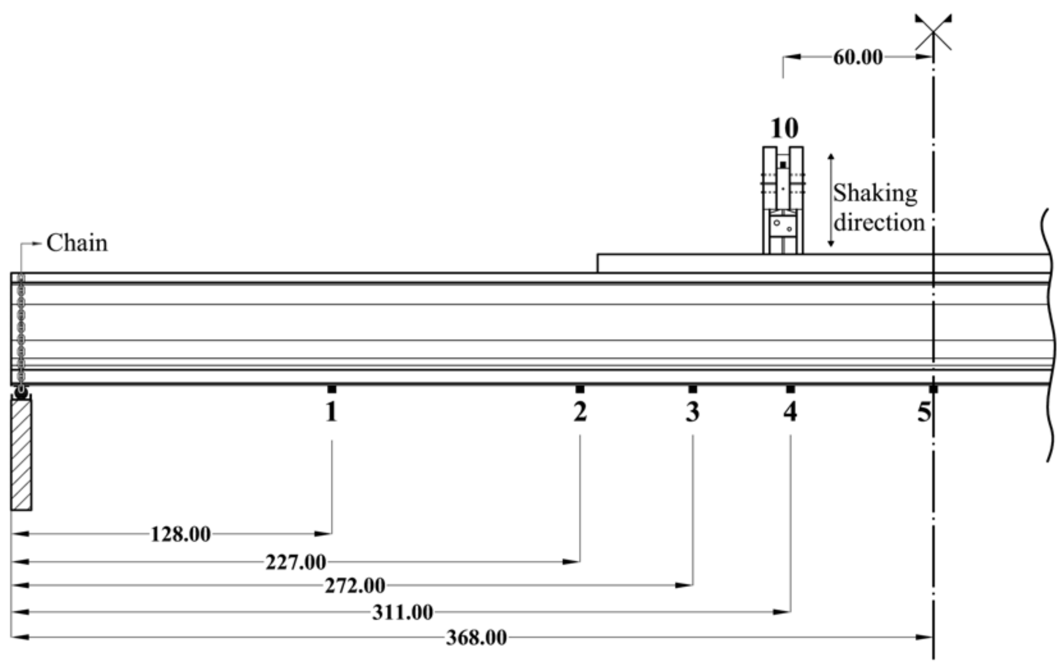

Figure 7. Sensors and shaker locations (all dimensions in inches).

5.2 Model updating results

The tested beam was modeled in MATLAB as a two-dimensional structure, discretizing the beam with 36 elements of variable lengths in order to account for sensors locations and the partial deck extensions. Figure 8 depicts the model discretization, in which F(t) indicates the force from the shaker.

The properties of the MATLAB model were estimated from the specimen's construction plans. This preliminary model is termed the non-updated model. The next step was to update the model using the measured structural responses. The data obtained from the test were filtered using a Chebyshev Type II low pass filter and then analyzed using the SSID algorithm. Next, the MATLAB model was updated to improve the frequency match. This was done by allowing the modification to the stiffness and mass terms of the elements by a factor ranging from 0.8 to 1.2. Thus, the damage indices α_i were expanded to include the modification to the stiffness and mass of the elements, denoted by β_i and γ_i, respectively. The optimization functions (i.e, Eqs. (44-46)) were solved using the particle swarm algorithm, yielding a new model, termed the updated model. Table 3 compares the retrieved frequencies from the SSID algorithm, with the frequencies from the non-updated model and the updated model. A comparison of the errors shows that the updated model resulted in a significant improvement in the modal parameters, reducing the maximum error on the frequencies from 4.3% to 1.8%. Figures 9 and 10 plots the modification factors for each element stiffness and mass, respectively.

Table 3. Fist three frequencies of the system, retrieved with SSID and calculated from the non-updated model.

mode	SSID frequencies (Hz)	non-updated model frequencies (Hz)	non-updated model error (%)	updated model frequencies (Hz)	updated model error (%)
1	7.06	6.92	1.96	7.04	0.28
2	25.09	25.91	-3.30	24.98	0.40
3	56.15	58.59	-4.30	57.17	-1.82

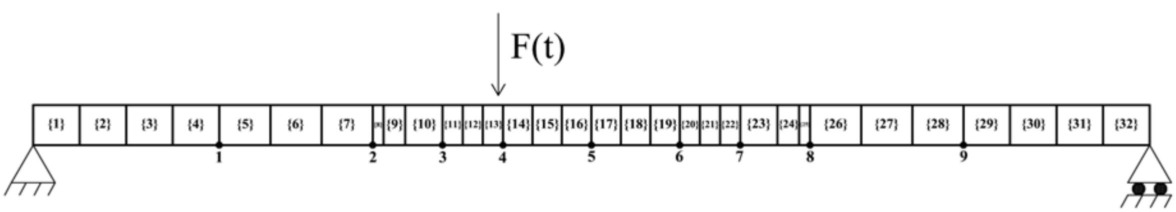

Figure 8. FE model discretization for the BTE60 specimen.

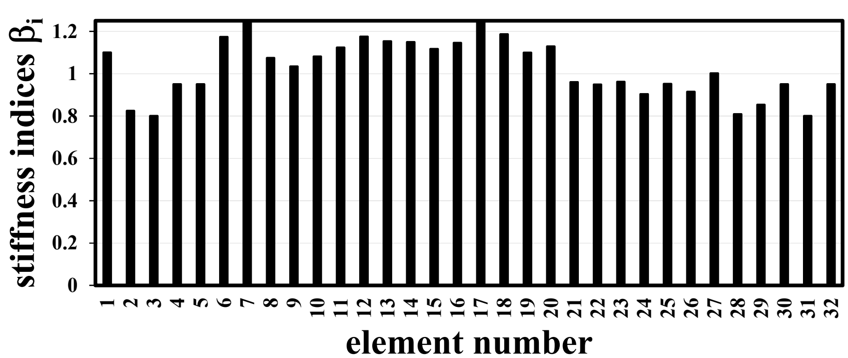

Figure 9. Modification factor β_i on the elements' stiffness.

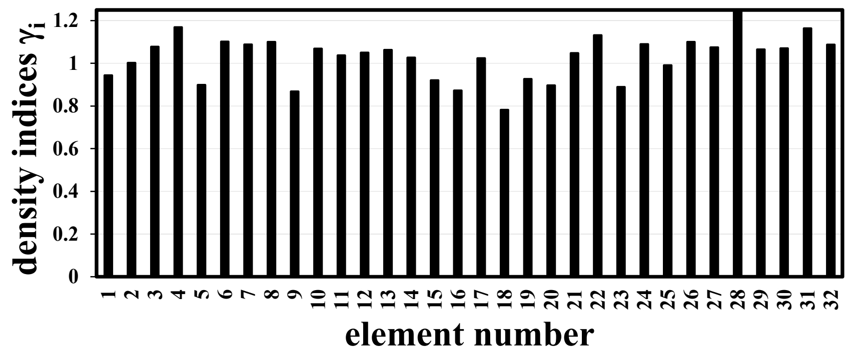

Figure 10. Modification factors γ_i on the elements' mass.

The resulting model was further validated by comparing the static displacement measurements acquired from string potentiometers during the application of a static load of 40 kips applied at the center of the beam. Figures 11 compares the static displacement obtained from the non-updated model, the updated model and the experimental data. Results show better agreement between the updated model and the experimental data, with an error of the maximum deflection at mid-span reducing from 5.1% to 0.2%.

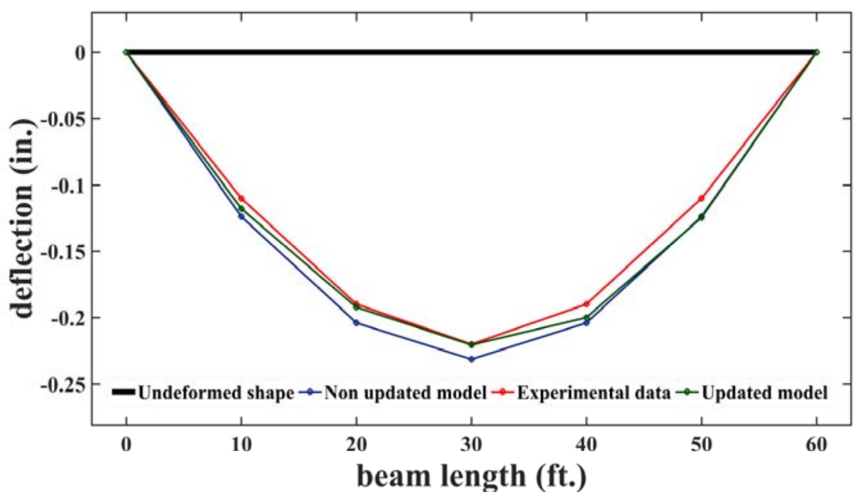

Figure 11. Comparison of the static deflection shapes.

6. CONCLUSIONS

This paper presented a technique for detecting, locating and quantifying damage that is based on the indirect reconstruction of reduced order stiffness matrices, using modal information retrieved through a stochastic subspace identification (SSID) technique. Retrieved modal properties were combined with a structural model which was, in turn, updated to match the modal data. This was done by generating optimization functions based on four performance criteria and solving them using a particle swarm algorithm.

The proposed approach was first successfully verified on numerically simulated data. Results show that the algorithm was able to detect, locate, and quantify damage with good accuracy. This was followed by a validation of the model using laboratory data collected from a full-scale PC beam excited with white noise. Results show that using the proposed approach, it was possible to reconstruct a model that matched the extracted modal parameters very well. This was further validated through the comparison of static displacement measurements obtained after application of a static load.

Overall, results presented in this paper show the promise of the proposed technique for detecting, locating, and quantifying damage using output-only data. Future work includes extended validation from experimental data that will include various damage levels and locations.

ACKNOWLEDGMENTS

This study is partly supported by grant #65A0586 from California Department of Transportation, and grant #1537626 from National Science Foundation. Any opinions, finding, and conclusion or recommendation expressed in this material are those of the authors and do not necessarily reflects the view of the sponsors.

REFERENCES

[1] Ubertini, F., Laflamme, S., Caylan, H., Materazzi, A. L., Cerni, G., Saleem, H., D'Alessandro, A., Corradini, A., "Novel nanocomposite technologies for dynamic monitoring of structures: a comparison between cement-based embeddable and soft elastomeric surface sensors," Smart Materials and Structures 23(4), 1-12 (2014).

[2] Laflamme, S., Cao, L., Chatzi, E., Ubertini, F., "Damage detection and localization from dense network of strain sensors," Shock and Vibration 2016, 1-13 (2016).

[3] Chinde, V., Cao, L., Vaidya, U., Laflamme, S., "Damage detection on mesosurfaces using distributed sensor network and spectral diffusion maps," Measurement Science and Technology 27(4), 1-13 (2016).

[4] Ranieri, C., Fabbrocino, G., "Automated output-only dynamic identification of civil engineering structures," Mechanical Systems and Signal Processing 24(3), 678-695 (2010).

[5] Peeters, B., De Roeck, G., "Reference-based stochastic subspace identification for output-only modal analysis," Mechanical Systems and Signal Processing 13(6), 855-878 (1999).

[6] Peeters, B., "System identification and damage detection in civil engineering structures," PhD thesis, Katholieke Universiteit Leuven, Belgium, (2000).

[7] Andersen, R., Brincker, R., Goursat, M., Mevel, L., "Automated modal parameter estimation for operational modal analysis of large systems," Proc. of the Second International Operational Modal Analysis Conference vol. 1, 299-308, (2007).

[8] Ubertini, F., Gentile, C., Materazzi, A. L., "Automated modal identification in operational conditions and its applications to bridges," Engineering Structures 46, 264-278 (2013).

[9] Peeters, B., De Roeck, G., "One-year monitoring of the Z24-Bridge: environmental effects versus damage events," Earthquake Engineering and Structural Dynamics 30, 149-171 (2001).

[10] Brownjohn, J. M. W., Carden, P., "Tracking the effects of changing environmental conditions on the modal properties of Tamar bridge," Porc. of the Third International Conference on Structural Health Monitoring of Intelligent Infrastractures, (2007).

[11] Ubertini, F., Comanducci, G., Cavalagli, N., " Vibration-based structural health monitoring of a historic bell-tower using output-only measurements and multivariate statistical analysis," Structural Health Monitoring 15(4), 438-457, (2016)

[12] Laflamme, S., Connor, J., [Structural Motion Engineering], Springer, New York, (2014).

[13] Zaiaedi-Rad, S., "Methods for updating numerical models in structural dynamics," PhD thesis, Imperial College of Science, Technology and Medicine, University of London, London, (1997).

[14] Alvin, K. F., Peterson, L. D., Park, K. C., "Method for determining minimum-order mass and stiffness matrices from modal test data," AIAA Journal 33(1), 1-8 (1995).

[15] Venter, G., Sobieszczanski-Sobieski, J., "Particle swarm optimization," AIAA Journal 41(8), 1-14 (2003).